Neuro-Oncology

25(9), 1563–1575, 2023 | https://doi.org/10.1093/neuonc/noad022 | Advance Access date 23 January 2023

Cancer-associated *SMARCAL1* loss-of-function mutations promote alternative lengthening of telomeres and tumorigenesis in telomerase-negative glioblastoma cells

Heng Liu, Cheng Xu, Bill H. Diplas, Alexandrea Brown, Laura M. Strickland, Haipei Yao, Jinjie Ling, Roger E. McLendon, Stephen T. Keir, David M. Ashley, Yiping He, and Matthew S. Waitkus

All author affiliations are listed at the end of the article

Corresponding Authors: Matthew S. Waitkus, 203 Research Drive, Medical Science Research Building 1, Room 181A, Duke University Medical Center, Durham, NC 27710, USA (matthew.waitkus@duke.edu); Yiping He, PhD, 203 Research Drive, Medical Science Research Building 1, Room 199A, Duke University Medical Center, Durham, NC 27710, USA (yiping.he@duke.edu).

Abstract

Background. Telomere maintenance mechanisms are required to enable the replicative immortality of malignant cells. While most cancers activate the enzyme telomerase, a subset of cancers uses telomerase-independent mechanisms termed alternative lengthening of telomeres (ALT). ALT occurs via homology-directed-repair mechanisms and is frequently associated with *ATRX* mutations. We previously showed that a subset of adult glioblastoma (GBM) patients with ATRX-expressing ALT-positive tumors harbored loss-of-function mutations in the *SMARCAL1* gene, which encodes an annealing helicase involved in replication fork remodeling and the resolution of replication stress. However, the causative relationship between SMARCAL1 deficiency, tumorigenesis, and de novo telomere synthesis is not understood.

Methods. We used a patient-derived ALT-positive GBM cell line with native SMARCAL1 deficiency to investigate the role of SMARCAL1 in ALT-mediated de novo telomere synthesis, replication stress, and gliomagenesis in vivo.

Results. Inducible rescue of SMARCAL1 expression suppresses ALT indicators and inhibits de novo telomere synthesis in GBM and osteosarcoma cells, suggesting that SMARCAL1 deficiency plays a functional role in ALT induction in cancers that natively lack SMARCAL1 function. SMARCAL1-deficient ALT-positive cells can be serially propagated in vivo in the absence of detectable telomerase activity, demonstrating that the SMARCAL1-deficient ALT phenotype maintains telomeres in a manner that promotes tumorigenesis.

Conclusions. SMARCAL1 deficiency is permissive to ALT and promotes gliomagenesis. Inducible rescue of SMARCAL1 in ALT-positive cell lines permits the dynamic modulation of ALT activity, which will be valuable for future studies aimed at understanding the mechanisms of ALT and identifying novel anticancer therapeutics that target the ALT phenotype.

Key Points

1. SMARCAL1 rescue in ALT+ cancers suppresses telomeric replication stress, prolongs survival of tumor-bearing mice, and inhibits telomeric DNA synthesis.
2. This study provides evidence that SMARCAL1 mutations are permissive to ALT and promote gliomagenesis.

Importance of the Study

Approximately 10%–15% of all solid tumors use alternative lengthening of telomeres (ALT) to maintain telomere length, and therapeutic strategies targeting ALT-mediated telomere synthesis is an area of significant translational and clinical interest. It is known that specific genetic mutations frequently co-occur with ALT (eg, ATRX, SMARCAL1), but the causal relationships between cancer-associated genetic mutations and ALT-mediated telomere synthesis are not well understood. Although *SMARCAL1* mutations are relatively rare compared to ATRX mutations, they provide a serendipitous opportunity to inducibly rescue SMARCAL1 expression in ALT+ cancers with native SMARCAL1 deficiency. Herein, we show that SMARCAL1 rescue in ALT+ cancers suppresses telomeric replication stress, prolongs the survival of tumor-bearing mice, and markedly reduces telomeric DNA synthesis. These studies provide conclusive evidence that cancer-associated *SMARCAL1* mutations are causative in ALT-mediated telomere synthesis and establish novel models for modulating the ALT phenotype, which will be valuable for identifying and testing novel anticancer drugs that target ALT.

Pathological telomere maintenance mechanisms occur in virtually all adult glioblastomas via the activation of telomerase or telomerase-independent mechanisms termed alternative lengthening of telomeres (ALT).[1–3] Approximately, 80% of adult GBM cases harbor single nucleotide mutations in the promoter region of the *TERT* gene (*TERT*p), which leads to the activation of telomerase.[1] A small subset of telomerase-positive *TERT*p-wild-type GBMs (~5%) activate *TERT* expression via chromosomal rearrangements upstream of the *TERT* gene.[2] The remaining cases maintain telomeres through ALT.[2] ALT utilizes homology-directed-repair mechanisms to maintain telomere length and is characterized by frequent alpha-thalassemia/mental retardation, X-linked (*ATRX*) loss-of-function mutations, high levels of DNA replication stress, and remodeling of telomeric chromatin to an epigenetic state that is permissive to homologous recombination.[4–9]

Loss-of-function mutations in the *ATRX* gene are well established to be associated with the ALT phenotype in adult and pediatric GBMs,[2,6,10,11] IDH-mutant astrocytomas,[12,13] high-grade astrocytomas with piloid features,[14,15] brainstem gliomas (including diffuse intrinsic pontine gliomas),[16,17] and several other cancer types, including sarcomas.[11] Mechanistically, loss of ATRX function is thought to contribute to ALT induction by dysregulating histone H3.3 deposition at telomeres, thus leading to increased DNA replication stress, formation of DNA double-strand breaks (DSBs), and telomere synthesis via break-induced replication.[18,19] Although *ATRX* mutations are closely associated with the ALT mechanism of telomere maintenance, there remains a substantial percentage of ALT-positive tumors that retain intact ATRX function and for which the mechanism of ALT induction and maintenance are not well understood.[9] In pediatric gliomas and other cancer types, such as pancreatic neuroendocrine tumors and osteosarcomas, ALT is also associated with loss-of-function mutations in *DAXX*, which encodes a protein that binds to ATRX to form a functional complex that mediates H3.3 deposition into heterochromatin.[6,11,20]

We previously reported that a subset of adult *IDH*-wild-type/*TERT*p-wild-type GBM patients harbor loss-of-function mutations in the *SMARCAL1* (SWI/SNF related, matrix associated, actin-dependent regulator of chromatin, subfamily a like 1) gene.[2] *SMARCAL1* encodes an annealing helicase that is recruited to stalled replication forks by replication protein A (RPA).[21] After being recruited to stalled forks by RPA, a single-stranded DNA binding protein, SMARCAL1 catalyzes fork regression in a manner that promotes fork stabilization and replication restart, thus preventing deterioration into DNA DSBs.[22,23] It has also been reported that SMARCAL1 deficiency is enriched in giant cell GBM tumors that exhibit the ALT phenotype.[24] In addition to GBM, *SMARCAL1* loss-of-function genetic alterations have been identified in ALT-positive sarcoma cell lines[2,25] and sarcoma clinical specimens,[26] as well as germline variants associated with pediatric sarcomas and central nervous system tumors.[27]

In the current study, we sought to investigate the functional role of *SMARCAL1* loss-of-function mutations in ALT-positive cancer cell lines with native SMARCAL1 deficiency. We used a patient-derived GBM cell line, D06MG, to establish the first orthotopic xenograft model of SMARCAL1-deficient ALT and to examine the effects of dynamically rescuing SMARCAL1 activity on the ALT phenotype. We found that SMARCAL1 activity suppresses phenotypic indicators of ALT, such as C-circles, and inhibits the formation of DNA DSBs at ALT-associated PML bodies (APBs) in G2-synchronized cell cultures. Inducible SMARCAL1 expression inhibited de novo telomere synthesis and was sufficient to suppress tumorigenicity in an orthotopic xenograft model. Our results demonstrate that cancer-associated *SMARCAL1* loss-of-function mutations are permissive to ALT-mediated telomere synthesis. Furthermore, these studies established valuable preclinical model systems that permit the dynamic modulation of ALT activity, which may be beneficial for ALT-specific drug screening and elucidating the mechanisms of ALT in future studies.

Materials and Methods

Cell Culture

Patient-derived neural stem cell cultures were passaged according to previously published methods[28] using the NeuroCult™ NS-A proliferation Kit (Stemcell™

Technologies, Cat#05751) supplemented with 20 ng/ml human recombinant EGF (Stemcell™ Technologies, Cat#78006.2) and 20 ng/ml human recombinant bFGF (Stemcell™ Technologies, Cat#78134.1). The D06MG cell line was established from archived tissue in the Preston Robert Tisch Brain Tumor Center Biorepository as previously described.[2] U2OS and Hela cells were purchased from Duke Cell Culture Facility. The NY cell line was purchased from the JCRB cell bank. U2OS cells were cultured in McCoy 5A containing 10% FBS, Hela cells were cultured in DMEM-HG containing 10% FBS, and NY cells were cultured in MEM containing 10% FBS. All culture media were purchased from ThermoFisher.

Xenograft Generation and Passaging

D06MG cells cultured under neural stem cell conditions were dissociated via Accutase digestion and mechanical trituration, filtered through a 70-μm filter, and resuspended in a methylcellulose PBS solution for injection into recipient mice. For initial subcutaneous xenograft generation, 5×10^6 cells were injected per animal. For intracranial injections from the D06MG-IC cell line, single-cell suspension was prepared in methylcellulose/PBS solution as described above and cells were injected into the right caudate nucleus, as previously described.[28]

Spectral Karyotyping Analysis

Spectral Karyotyping preparation and analysis were performed according to established procedures by Herbert Irving Comprehensive Cancer Center Cytogenetics Core, Columbia University. Cells were cultured attached in laminin-coated plates with serum-free medium and treated with 0.05 μM colcemid solution for 2 hours. Medium-containing floating cells were collected, spun down, and treated with 0.56% KCl hypotonic solution for 20 minutes at 37°C. Cells were fixed with methanol/acetic acid (3:1 by volume) fixative solution and dropped to ethanol-cleaned slides. After pretreatment with pepsin solution, the slides were denatured and hybridized with chromosome-specific painting probes at 37°C for 48 hours. Probes were visualized using Cy5-conjugated avidin and Cy5.5-conjugated anti-mouse IgG. Chromosomes were counterstained with 4,6-diamidino-2-phenylindole. 20 metaphases from each cell line were randomly selected and analyzed.

Immunoblotting

Cells were lysed in RIPA buffer (Millipore Sigma, Cat# R0278) with 1× protease inhibitor cocktail (Cell Signaling Technology, Cat# 5871S). Protein lysates containing ~20 μg total protein were loaded and resolved using (4%–12%) NuPAGE Bis-Tris gradient gel. Gels were soaked in protein transfer buffer (48 mM Tris, 39 mM glycine, 10% methanol, 0.0375% SDS) and transferred to a PVDF membrane using a BioRad Mini Tran-Blot transfer cell. After transfer to PVDF membranes, membranes were blocked with Pierce TBST protein-free blocking buffer (Cat # 37572) and blotted with antibodies diluted in blocking buffer. Antibodies used included anti-ATRX (cell signaling, #14820), anti-DAXX (cell signaling, #4533), anti-SMARCAL1 (cell signaling, #44717), and anti-GAPDH (Santa Cruz, sc-47724).

Telomerase PCR ELISA Assay

The activity of telomerase in the cell lines was detected using the TeloTAGGG telomerase PCR ELISA Kit (Roche, Cat# 12013789001). The assay was performed according to the manufacturer's instructions and repeated in triplicate. 2×10^5 cultured cells were collected, counted and lysed in 200μL lysis reagent. One microliter of cell lysis, negative controls, and positive controls were mixed with 25 μL TRAP Reaction buffer. The reaction products were hybridized to the microplate precoated with digoxigenin (DIG)-labeled telomere probes, incubated with anti-DIG-POD antibody and detected by TMB substrate solution. Data were collected by measuring absorbance of the samples at 450 nM with a reference wavelength of 650 nM using Tecan i200 Pro plate reader.

RNA-Seq

Cell line RNA was extracted using Maxwell RSC simplyRNA Cells Kit (Promega Cat# AS1390). Extracted RNA was sent to Novogene (San Diego, CA, USA) for quality control and RNA sequencing. The raw FASTQ data were aligned to the reference genome (GRCh38/hg38) using HISAT2.[29] Count reads were mapped to genes using feature Count and DESeq2 was used for count normalization.[30,31] Limma-voom was used for differential gene analysis.[29] EGSEA was used for gene set enrichment analysis.[32] A false discovery rate cutoff of 0.05 of differentially expressed genes was used for the calculation of significance score and regulation direction. Data are available under the GEO accession number GSE214466.

Immunofluorescence-FISH Co-staining

Cells were grown on 3-well chamber slides to subconfluence and fixed with 4% formaldehyde, washed with PBS, and then incubated with primary antibodies in blocking buffer (1 mg/mL BSA, 3% goat serum, 0.1% Triton X-100, and 1 mM EDTA) overnight at 4°C. Slides were incubated with goat secondary antibodies against rabbit or mouse IgG, conjugated with AlexaFluor-488 or 594 (ThermoFisher, 1:500). Cells were then rinsed with PBS and fixed with 2% formaldehyde for 10 minutes at room temperature, followed by a series of dehydration steps (70%, 95%, and 100%) ethanol. Slides were incubated with TelC-Cy3 (PNA Bio, #F1002) or TelC-AlexaFlour-647 (PNA Bio, #F1013) 1:1000 in hybridizing solution, denatured at 70°C for 10 minutes on a ThermoBrite instrument, and then incubated at room temperature for 2 hours or overnight at 4°C. Slides were washed with 70% formamide, 10 mM Tris–HCl, PBS, stained with DAPI, and coverslipped and sealed. Slides were imaged on a Zeiss 880 upright/inverted confocal microscope and a Zeiss 780 upright confocal microscope, and images were analyzed using Zen

software. The Focinator program was used to quantitate foci and colocalization of IF-stained foci with telomeres.[33] Antibodies used included γH2AX (Cell Signaling, Cat # 9718), PML (Santa Cruz, Cat #sc-966), and BLM (Santa Cruz, Cat#365753).

Nascent Telomere DNA Synthesis Labeling and Pull Down

The ALT telomere DNA synthesis assay (ATSA assay) was performed as previously described.[34] Doxycycline-treated (0.5 μg/ml, 5 days) and control cells were seeded into chamber slides and synchronized to late G2 phase using Thymidine and CDK1 inhibitor, RO-3306 2-step synchronization. Cells were pulse-labeled with 10 μM 5-ethynyl-2′-deoxyuridine (EdU) for 2 hours, permeabilized, and fixed with 4% formaldehyde in PBS. EdU-incorporated cells were stained by Click-iT chemistry (ThermoFisher) to detect the incorporated EdU, followed by IF-FISH staining using a TelC-Cy3 probe and antibodies against PML, EdU, and γ-H2AX. For BrdU (5-bromo-2′-deoxyuridine) pulldown assays, cells were pulsed with 10 μM BrdU for 2 hours and then lysed for genomic DNA isolation using a Promega Maxwell, RSC Cultured Cells DNA kit. DNA was sonicated, immunoprecipitated using an anti-BrdU antibody (BD-Biosciences, Cat # 347580), dot-blotted onto a nylon membrane, and detected by biotin-labeled telomere probe and quantified using BioRad densitometry software.

Mouse Intracranial Injection

Glioma stem-like cells were transplanted into the right caudate nucleus of athymic nude mice (1×10^5 cells per injection, $N = 8$ per group). Mice were placed in a Stoelting stereotactic injection device under isoflurane-induced anesthesia. Cells were injected 2 mm right and 3.5 mm deep relative to Bregma using a 25-gauge needle. After recovery from injections, animals were monitored for the onset of neurological symptoms as evidenced by indicators such as inability to ambulate, agonal breathing, head tilting or doming, or a 20% loss of body weight, and then euthanized. Differences in survival of tumor-bearing mice between conditions were evaluated using the log-rank test.

Statistical Analyses

For analyzing differences between doxycycline-treated or untreated cells, a student's *t*-test was used. For c-circle assays with >2 groups, a one-way analysis of variance was used with correction for multiple comparisons by the Bonferroni method. Survival analyses for in vivo animal studies were performed using the log-rank test. For gene expression analyses via RNA-seq, a cutoff of false discovery rate 0.05 of differentially expressed genes was used for the calculation of significance score and regulation direction. For figures and figure legends in the manuscript, the following annotation is used to denote varying thresholds of statistical significance: $^*P < .05$. $^{**}P < .01$. $^{****}P < .0001$. ns = nonsignificant.

Whole-Exome Sequencing

Whole-exome sequencing of D06MG cell line genomic DNA was performed at Azenta Life Sciences. Sequencing libraries were prepared using the Twist Human Core Exome Kit. Sequencing was performed on an Illumina HiSeq 4000 instrument. Raw sequencing data were evaluated with FASTQC 0.11.9. Sequencing adapters and low-quality bases were trimmed using Trimmomatic 0.39. Cleaned reads were then aligned to the GRCh38 reference genome using Sentieon 202112.01. Alignments were sorted and PCR/Optical duplicates were marked. Somatic SNVs and small INDELs were called using Sentieon 202112.01 (TNseq algorithm). The VCF files generated by the pipeline were then normalized (left alignment of INDELs and splitting multiallelic sites into multiple sites) using bcftools 1.13. Overlapped transcripts were identified for each variant and the effects of the variants on the transcripts were predicted by Ensembl VEP 104. Data are available in the sequencing read archive under the BioProject PRJNA923134.

Results

A Primary SMARCAL1-Deficient GBM Culture Displays Stable Indicators of ALT Activity Following In Vivo Propagation

We first sought to develop a GBM xenograft from a previously established patient-derived cell line that was shown to be ALT-positive and SMARCAL1 deficient.[2] This cell line, termed D06MG, was established from a primary, untreated GBM tissue following surgical resection. The primary tumor was defined to be *TERT* promoter wild type, IDH1/2 wild type, and retained nuclear ATRX expression via immunohistochemistry (Supplemental Table 1).[2] The patient-derived parental D06MG cells were grown in serum-free neural stem cell media as neurospheres (hereafter termed D06MG- neural stem cell) and showed stable SMARCAL1 deficiency and maintained expression of ATRX and DAXX over several serial passages (Figure 1A). Immunofluorescence and fluorescence in situ hybridization co-staining (IF-FISH) for PML and TelC respectively showed that D06MG- neural stem cell cells exhibit readily detectable ALT-APBs, consistent with a stable ALT phenotype and telomere length maintenance via ALT (Figure 1B).

We then sought to determine whether D06MG cells were tumorigenic in vivo and to establish xenografts from this cell line. D06MG-NSC cells were subcutaneously implanted into inbred nude mice and allowed to form xenografts over time (Supplementary Figure 1A). Subcutaneous tumors formed with a latency of approximately 180 days (Supplementary Figure 1A, B). Explanted tissue from subcutaneous xenografts was then used to establish a stable cell line under neurosphere growth conditions in cell culture (D06MG-SubQ). In addition, tissue from subcutaneous xenografts was directly passaged forward via intracranial injections into recipient nude mice (Supplementary Figure 1A). Orthotopic tumors formed with an approximate latency of 160 days after intracranial transplantation and explanted cells from these tumors were collected and used to establish a cell line in culture (D06MG-IC). These studies

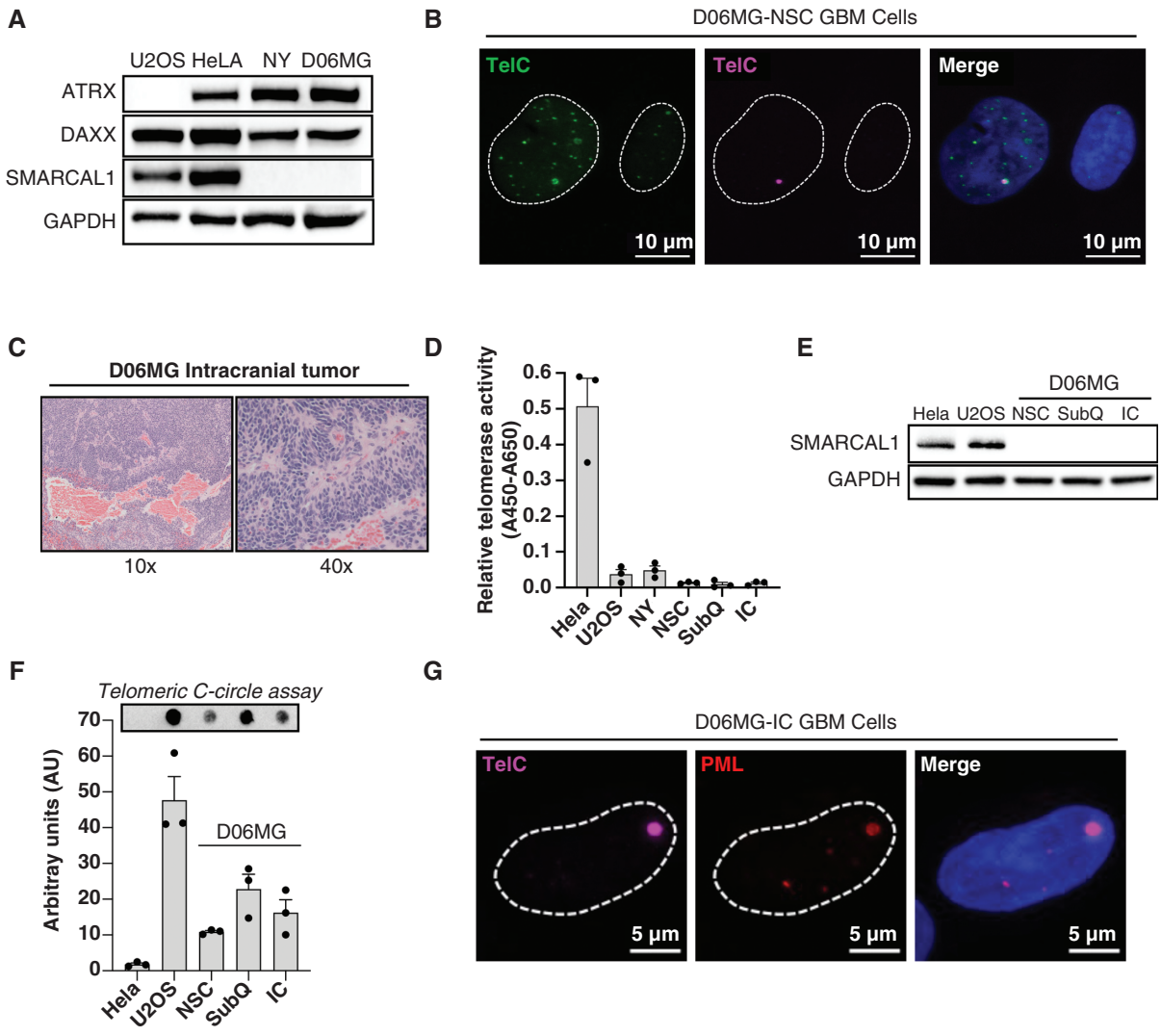

Figure 1. D06MG tumor cells maintain alternative lengthening of telomeres features after in vivo propagation. (**A**) Western blot detection of ATRX, DAXX, and SMARCAL1 proteins. U2OS (osteosarcoma), HeLa (endocervical adenocarcinoma) and NY (osteosarcoma) cells were used for positive and negative controls for ATRX and SMARCAL1 detection. (**B**) IF-FISH analysis of D06MG-NSC cells for detection of telomeric foci and nuclear PML foci. (**C**) H&E staining of formalin-fixed paraffin-embedded orthotopic D06MG tumor tissue using 10x and 40x objectives. (**D**) TeloTAGG assay for the detection of telomerase activity between cell lines. HeLa and U2OS were included as positive and negative controls for telomerase activity, respectively. Three independent replicates are shown for each condition and the error bars represent the mean +/- standard deviation. (**E**) Western blot for the detection of SMARCAL1 protein from D06MG cell lines, as well as positive controls HeLA and U2OS. (**F**) C-circle assay for the detection of extrachromosomal circular telomeric repeats. Three independent replicates are shown for each condition and the error bars represent the mean +/– standard deviation. (**G**) Confocal imaging using a 63x objective of IF-FISH co-staining for telomeric DNA using a TelC-AlexaFlour-647 probe and an anti-PML antibody.

demonstrated the in vivo tumorigenicity of the D06MG-NSC primary culture and established additional xenograft-derived cell lines from the subcutaneous and orthotopic tumors (Figure 1C).

Similar to the parental D06MG-NSC cell line, cell lines obtained from the subcutaneous and orthotopic tumors exhibited low or undetectable telomerase activity (Figure 1D), demonstrating that the intrinsic ALT activity of D06MG is sufficient to maintain telomeres in a manner that promotes tumorigenesis. D06MG-SubQ and D06MG-IC lines were SMARCAL1 deficient (Figure 1E) and displayed ALT indicators, including the presence of extrachromosomal C-circles (Figure 1F) and APBs (Figure 1G), demonstrating that the ALT phenotype is maintained in these cells after in vivo propagation. In addition, whole exome sequencing of the D06MG-NSC, D06MG-SubQ, and D06MG-IC lines showed that the genetic driver mutations observed in the original patient tumor (Supplementary Table 1) were maintained in all sub-lines, including the SMARCAL1^{W479X} mutation, an *NF1* mutation encoding a R192X nonsense variant, and conserved missense mutations in PTEN (M35V) and PIK3R6 (G585D)

(Supplementary Dataset 1). Copy number variation analyses using WES data did not identify any recurrent CNVs in specific genes between the D06MG-NSC lines and the D06MG-SubQ orD06MG-IC sub-lines (Supplementary Dataset 2).

Because SMARCAL1 is involved in the maintenance of genome integrity and stability,[21] we analyzed the karyotypes of D06MG cell lines before and after propagation as xenografts in vivo. We found that all D06MG cell lines (prior to and post in vivo growth) displayed mostly diploid karyotypes (Figure 2A, B, Supplementary Dataset 3). While triploid and tetraploid metaphase spreads were identified in the parental D06MG-NSC culture, D06MG-SubQ and D06MG-IC showed a trend toward a slightly reduced overall number of chromosomes, as well as a lack of triploid or tetraploid cells after in vivo tumorigenesis and propagation (Figure 2C). All metaphase spreads analyzed from both D06MG-SubQ and D06MG-IC showed chromosomal translocations between chromosomes 4 and 22 [(4;22)(q11;q10)] and additional abnormal copies of chromosome 7 (Figure 2B, Supplementary Dataset 3). These distinct alterations were absent in metaphase spreads of D06MG-NSC, suggesting that there was a clonal expansion of a specific tumorigenic subclone following the initial in vivo propagation of D06MG-NSC.

Transcriptomic Analyses Identify Gene Expression Programs Associated With Tumorigenesis in D06MG Xenografts

To determine the gene expression differences associated with the establishment of subcutaneous and intracranial tumors of D06MG, we performed transcriptomic profiling (mRNA-seq) on the D06MG-NSC parental cells, D06MG-SubQ, and the D06MG-IC cells that were explanted and established as distinct sub-lines in cell culture. We noted that in comparison to parental D06MG-NSC cells, D06MG-IC, and D06MG-SubQ cells displayed remarkably similar pathway-level gene expression changes using the Hallmark pathway analysis.[35] These changes include the modulation of cell cycle gene expression, including the G2M checkpoint, mitotic spindle, the E2F pathway, and the p53 pathway (Supplementary Figure 2A–B, Dataset 4). Furthermore, D06MG cells undergoing in vivo propagation exhibited higher expression of genes in the hypoxia response pathway, as well as genes related to glycolysis, potentially indicating their adaption to in vivo

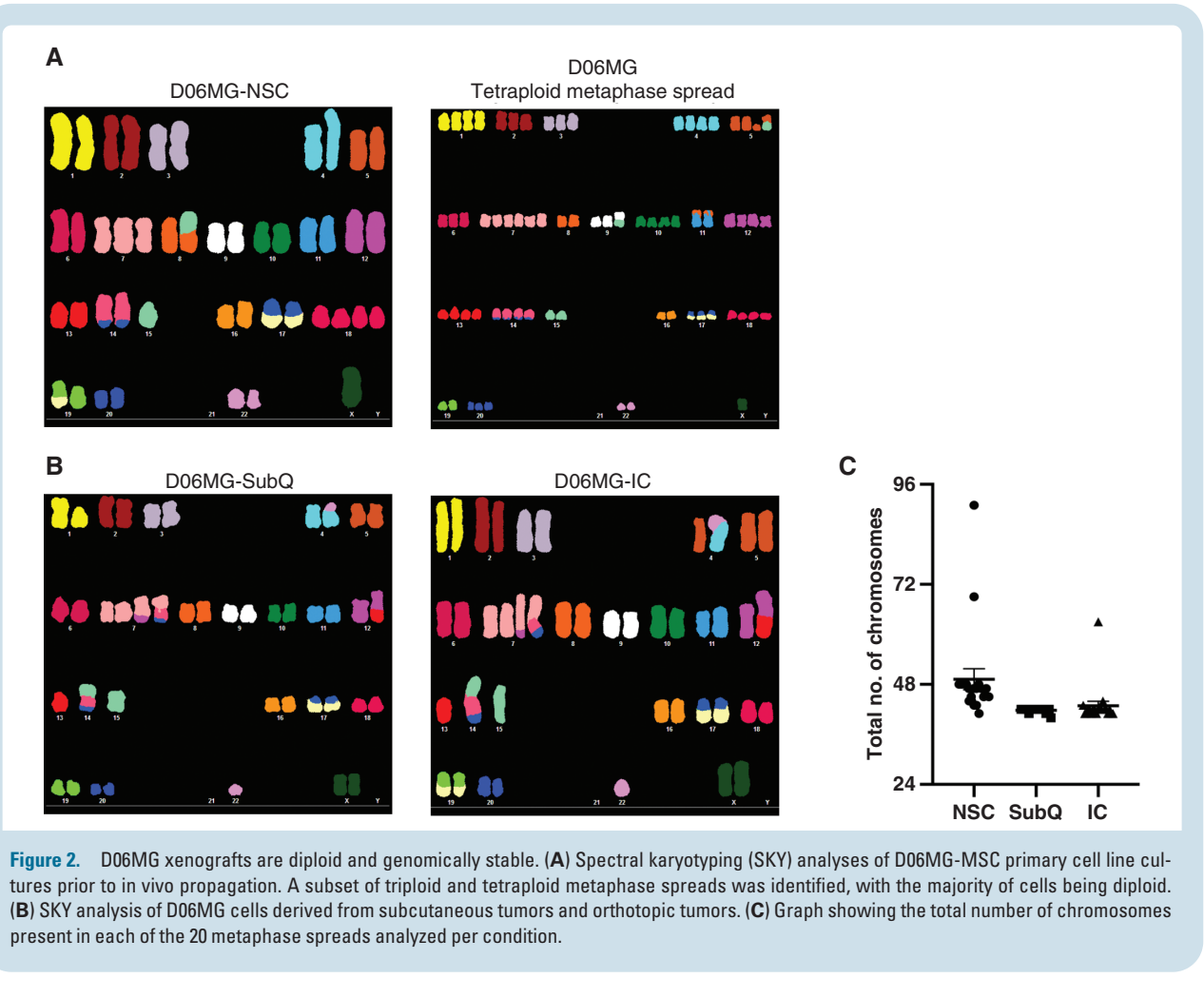

Figure 2. D06MG xenografts are diploid and genomically stable. (**A**) Spectral karyotyping (SKY) analyses of D06MG-MSC primary cell line cultures prior to in vivo propagation. A subset of triploid and tetraploid metaphase spreads was identified, with the majority of cells being diploid. (**B**) SKY analysis of D06MG cells derived from subcutaneous tumors and orthotopic tumors. (**C**) Graph showing the total number of chromosomes present in each of the 20 metaphase spreads analyzed per condition.

growth (Supplementary Figure 2A–B, Dataset 4). We next compared the gene expression changes in the D06MG-IC cells relative to the D06MG-SubQ cells. Gene expression changes in the most significantly altered set of genes were those related to the epithelial-to-mesenchymal transition pathway (Supplementary Figure 2C). While both D06MG-IC and D06MG-SubQ showed decreased expression of epithelial to mesenchymal transition genes relative to the parental cell lines, the extent of epithelial to mesenchymal transition gene downregulation was greater in D06MG-IC cells (Supplementary Figure 2C, Dataset 4).

We then examined the differential regulation of genes previously reported to be involved in telomere maintenance or telomere localization in ALT-positive cells. To this end, we used a list of genes encoding for proteins

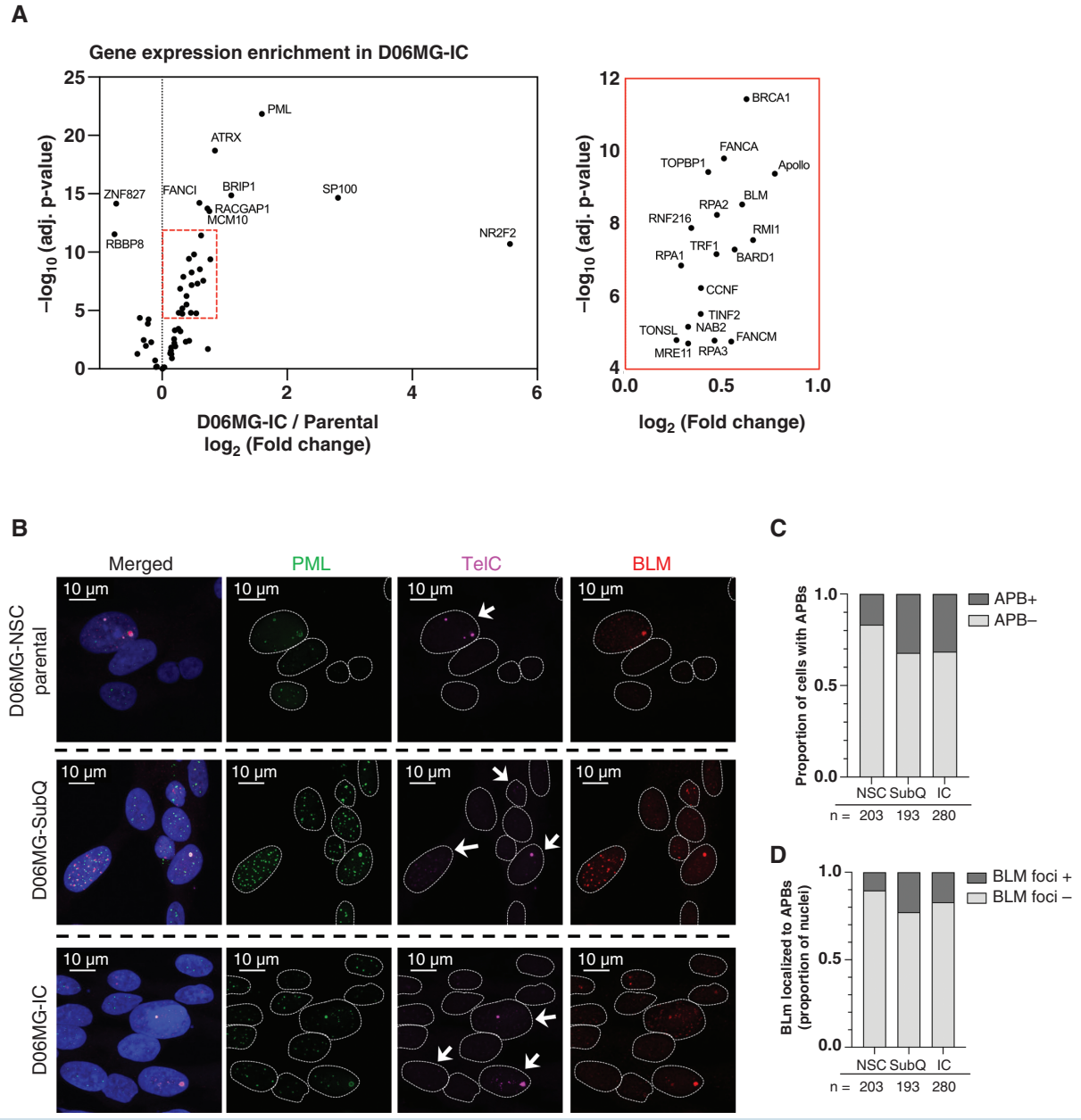

Figure 3. Enrichment of alternative lengthening of telomeres (ALT)-associated gene expression and associated PML bodies (APBs) in D06MG-SubQ and D06MG-IC lines. (**A**) Volcano plot of genes encoding proteins localized to ALT telomeres plotted by log2 fold change and adjusted *P*-value when comparing mRNA expression of D06MG-IC cells relative to D06MG-NSC. The red dashed box indicates the expanded portion of the plot visualized to the right. Gene identifiers are labeled next to the individual data points. (**B**) IF-FISH staining of D06MG cell lines cells with antibodies to PML and BLM, costained with a TelC-647 telomere probe and counterstained with DAPI. Dashed lines represent the location of nuclei and white arrows note the presence of BLM-positive APBs in selected cells. (**C**) Quantitation of the proportion of nuclei that contain an APB in each cell line. (**D**) Quantitation of the proportion of nuclei with APBs that exhibit colocalization with nuclear BLM foci.

that have been shown to localize to ALT telomeres using proteomic analyses in U2OS cells.[36] We also included *ATRX* because the previously published proteomic analysis was conducted in ATRX-deficient cells, rather than SMARCAL1-deficient cells that have intact ATRX expression (ie, D06MG). Comparing the expression of these ALT telomere-associated genes, we observed that there was a trend toward increased mRNA expression of genes associated with ALT in D06MG-IC cells, including ATRX, PML, FANCM, RPA1/2, and BLM (Figure 3A). While the overwhelming trend was toward increased expression of these ALT-associated genes, there was also a notable decrease in expression of RBBP8 and ZNF827 (Figure 3A). To investigate whether this enrichment in ALT-associated gene expression was evident at the protein level, we performed IF-FISH analyses to assess the abundance of APBs in these cell lines (Figure 3B, C). We found that there was a general enrichment of APBs in the D06MG-SubQ and D06MG-IC lines relative to the parental line (Figure 3C). Due to the previously reported roles of BLM at ALT telomeres,[37] we also asked whether the observed increase in BLM mRNA expression coincided with increased BLM localization to APBs in D06MG-SubQ and D06MG-IC. We found that a subset of APBs exhibited clear localization of BLM foci in all of the D06MG cell lines and that the differences between lines reflected the general increase in APBs, suggesting that the enrichment in BLM expression is a reflection of increased APB abundance rather than a specific regulation of BLM *per se* (Figure 3D).

SMARCAL1 Deficiency Promotes ALT-mediated Telomere Synthesis and Orthotopic Tumorigenesis

We previously reported that SMARCAL1 deficiency was associated with ALT in a subset of adult GBM cases and the CAL-78 chondrosarcoma cell line.[2] In addition, we showed that SMARCAL1 rescue suppressed phenotypic indicators of ALT, including C-circles and ultrabright telomeric foci.[2] We, therefore, sought to assess the functional role

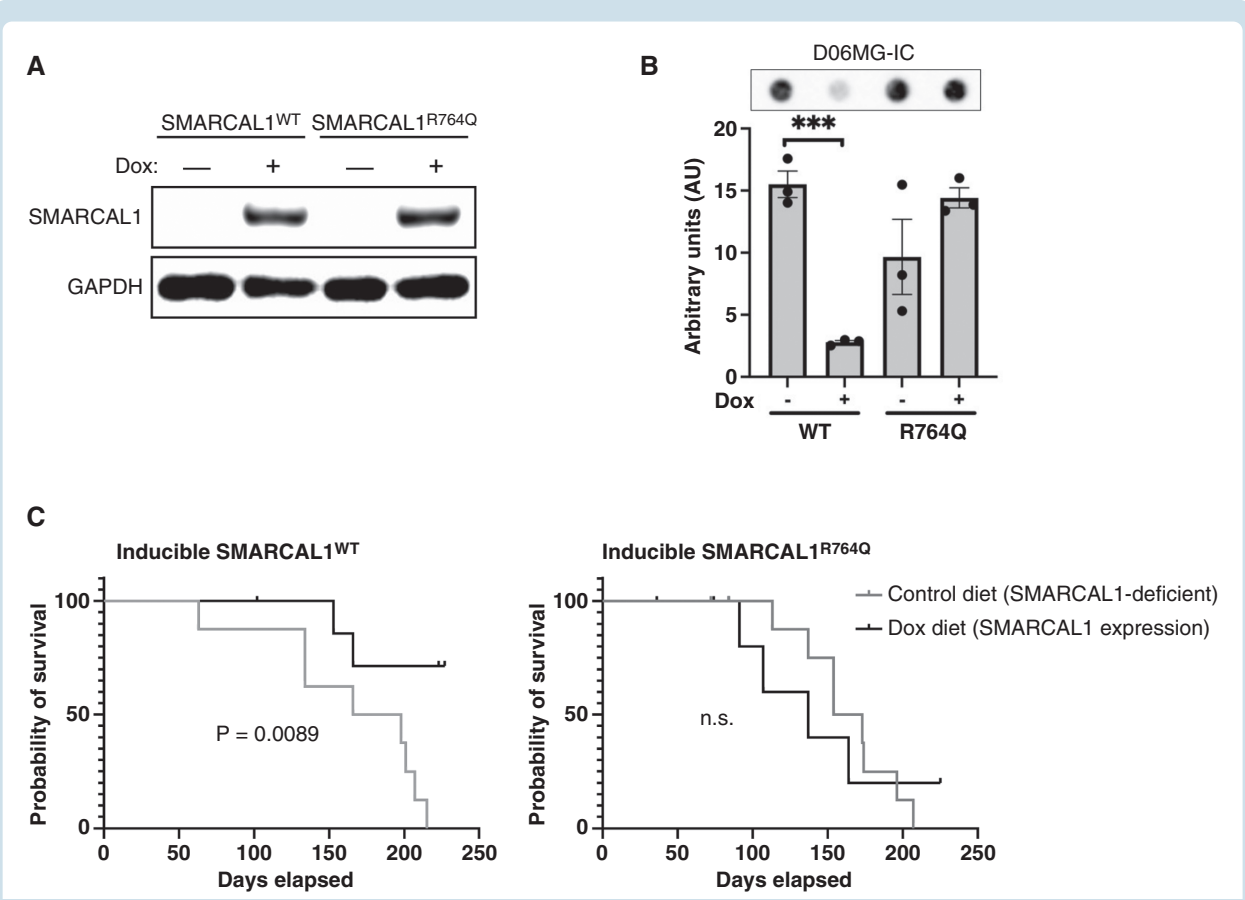

Figure 4. Inducible SMARCAL1 rescue suppresses alternative lengthening of telomeres indicators and in vivo tumorigenesis. (**A**) Western blot analyses measuring doxycycline-inducible expression of SMARCAL1^{WT} or SMARCAL1R764Q in D06MG-IC. (**B**) C-circle analysis of D06MG-IC without or with doxycycline-induced expression (5 days) of SMARCAL1^{WT} or SMARCAL1^{R764Q}. Differences between conditions were assessed using a student's *t*-test. (**C**) D06MG-IC cells with inducible SMARCAL1^{WT} (left panel) were orthotopically implanted into mice. 5 days after implantation, mice were switched to a control or doxycycline-containing chow diet, and their survival was determined according to loss of body weight and/or the onset of neurological symptoms. The same experimental framework was used for orthotopic tumors expressing doxycycline-inducible SMARCAL1^{R764Q} as a control to account for possible effects of doxycycline chow (right panel). Survival differences between groups were analyzed via the log-rank test.

of SMARCAL1 deficiency in promoting ALT. To this end, we utilized a doxycycline-inducible expression system that permits the controlled expression of transgenic SMARCAL1^{WT} or SMARCAL1^{R764Q}, a catalytically inactive mutant[2,21,38] (Figure 4A). Notably, this type of inducible rescue in ATRX-deficient ALT models (eg, U2OS, SaOS2) has been historically challenging due to the large size of the ATRX protein. On the other hand, the relatively low molecular weight of SMARCAL1 makes the inducible rescue approach feasible and allows for dynamic control of ALT phenotypes (Figure 4A).

Using this model, we found that inducible SMARCAL1 rescue suppressed the abundance of extrachromosomal telomeric C-circles (Figure 4B), consistent with previous observations and validating the functional rescue of SMARCAL1 activity. We then sought to determine the extent to which SMARCAL1 deficiency regulates tumorigenesis in vivo using orthotopic D06MG-IC tumors with or without doxycycline-induced SMARCAL1 rescue. D06MG-IC cells were transduced with lentiviral particles containing a doxycycline-inducible expression vector for SMARCAL1^{WT} or SMARCAL1^{R764Q}. After orthotopic transplantation of these isogenic GBM cell lines into mice, we used a doxycycline-containing diet to induce the expression of SMARCAL1 in vivo. We found that the restoration of SMARCAL1 expression prolonged survival in tumor-bearing mice and decreased the overall penetrance of tumorigenesis (Figure 4C). These SMARCAL1-mediated effects were not observed in the SMARCAL1^{R764Q} mutant condition, suggesting that SMARCAL1 ATPase activity is critical for suppressing tumorigenesis in these cells and ruling out potential effects of doxycycline in vivo (Figure 4D). Collectively, these results demonstrate a functional role of SMARCAL1 deficiency in ALT-mediated telomere synthesis and highlight the importance of this telomere maintenance mechanism in the subset of ALT-positive cancers that exhibit SMARCAL1 loss-of-function.

To gain insight into the mechanism by which SMARCAL1 suppresses orthotopic tumorigenesis in this model, we used inducible SMARCAL1 rescue to investigate the dynamic modulation of ALT indicators and de novo telomere synthesis in D06MG-IC cells. Because ALT utilizes break-induced replication for maintaining telomere length, we examined the regulation of APBs and the colocalization of γH2AX (a marker of DNA DSBs) in APBs in G2/M-synchronized cells. We found SMARCAL1 expression led to a reduction in APBs that colocalized with γH2AX (Figure 5A). This result suggests that SMARCAL1 expression suppresses replication stress and inhibits the formation of DSBs at telomeres in G2/M phase and is consistent with a role of SMARCAL1 in facilitating replication fork repair and restart to prevent degeneration into DSBs.[21,22,39]

We then investigated whether SMARCAL1 loss-of-function is necessary for de novo telomere synthesis in ALT+ cell lines with native SMARCAL1 deficiency. These experiments used D06MG-IC cells and NY cells, an osteosarcoma cell line previously shown to be SMARCAL1-deficient and ALT-positive.[25] Similar to D06MG, NY cells are C-circle-positive at baseline, and SMARCAL1 rescue significantly reduces C-circle abundance in these cells (Supplementary Figure 3A–B). We then used EdU pulse-labeling of de novo DNA synthesis in late G2-synchronized D06MG-IC and NY cells and examined the colocalization of newly synthesized DNA with APBs. Doxycycline-inducible rescue of SMARCAL1 expression significantly inhibited the number of EdU+ APBs relative to cells without SMARCAL1 rescue in both D06MG-IC cells and NY cells, demonstrating that SMARCAL1 activity suppresses de novo telomere synthesis in these lines (Figure 5B, C). To validate this finding, we performed a BrdU pulse-labeling experiment to label newly synthesized DNA and subsequently immunoprecipitated BrdU-labeled DNA for telomere probe detection via dot blot. SMARCAL1 rescue significantly inhibited the amount of BrdU-incorporated telomeric c-strand DNA relative to SMARCAL1 deficient controls (Supplementary Figure 3C).

Discussion

In this study, we used a patient-derived ALT-positive GBM cell line with native SMARCAL1 deficiency to establish subcutaneous and orthotopic xenografts, as well as cell lines derived from the xenograft tissue. Using an inducible rescue of SMARCAL1 expression, we found that SMARCAL1 activity suppresses ALT indicators and inhibits de novo telomere synthesis (Figure 5A–C, Supplementary Figure 3C), suggesting that SMARCAL1 deficiency plays a functional role in ALT induction in cancers that natively lack SMARCAL1 function.

Our in vivo results demonstrate that the functional reconstitution of SMARCAL1 activity suppressed tumorigenesis and prolonged the survival of tumor-bearing mice (Figure 4C). However, tumorigenesis and the onset of neurological symptoms were still observed in a subset of mice with SMARCAL1 rescue. Future studies will investigate the mechanisms by which these tumors arise. One possibility is that they arise due to phenotypic plasticity; whereby, the arising tumors have activated telomerase or maintain ALT by a compensatory mechanism in the presence of SMARCAL1 rescue. Another possibility is that the doxycycline-inducible rescue of SMARCAL1 was insufficient to fully suppress telomere synthesis in these tumors.

Our results establish SMARCAL1 as an additional gene associated with the onset of the ALT phenotype. In cancer, loss-of-function genetic alterations in *ATRX* or *DAXX*, which encode histone H3.3 chaperone proteins, are well established to play a role in ALT-mediated telomere maintenance in cancers from several tissue types that are enriched for ALT-positive tumors.[7,11] In addition, cell-based studies have shown that depletion of another histone chaperone, ASF1, leads to rapid induction of ALT and suppression of telomerase activity.[40] It is notable that the ATRX/DAXX complex and ASF1 function as histone chaperones, while SMARCAL1 functions as an annealing helicase that is recruited to stalled replication forks with lagging strand gaps by the single-stranded binding protein RPA.[21,41,42] SMARCAL1, therefore, joins a growing list of proteins, including SLX4IP and TOP3A, whose altered activity is associated with ALT but do not have a direct role in H3.3 deposition.[26,43] In this way, it remains unclear whether the mechanisms by which SMARCAL1 loss-of-function leads to ALT are similar to, or distinct from, the mechanisms of ALT

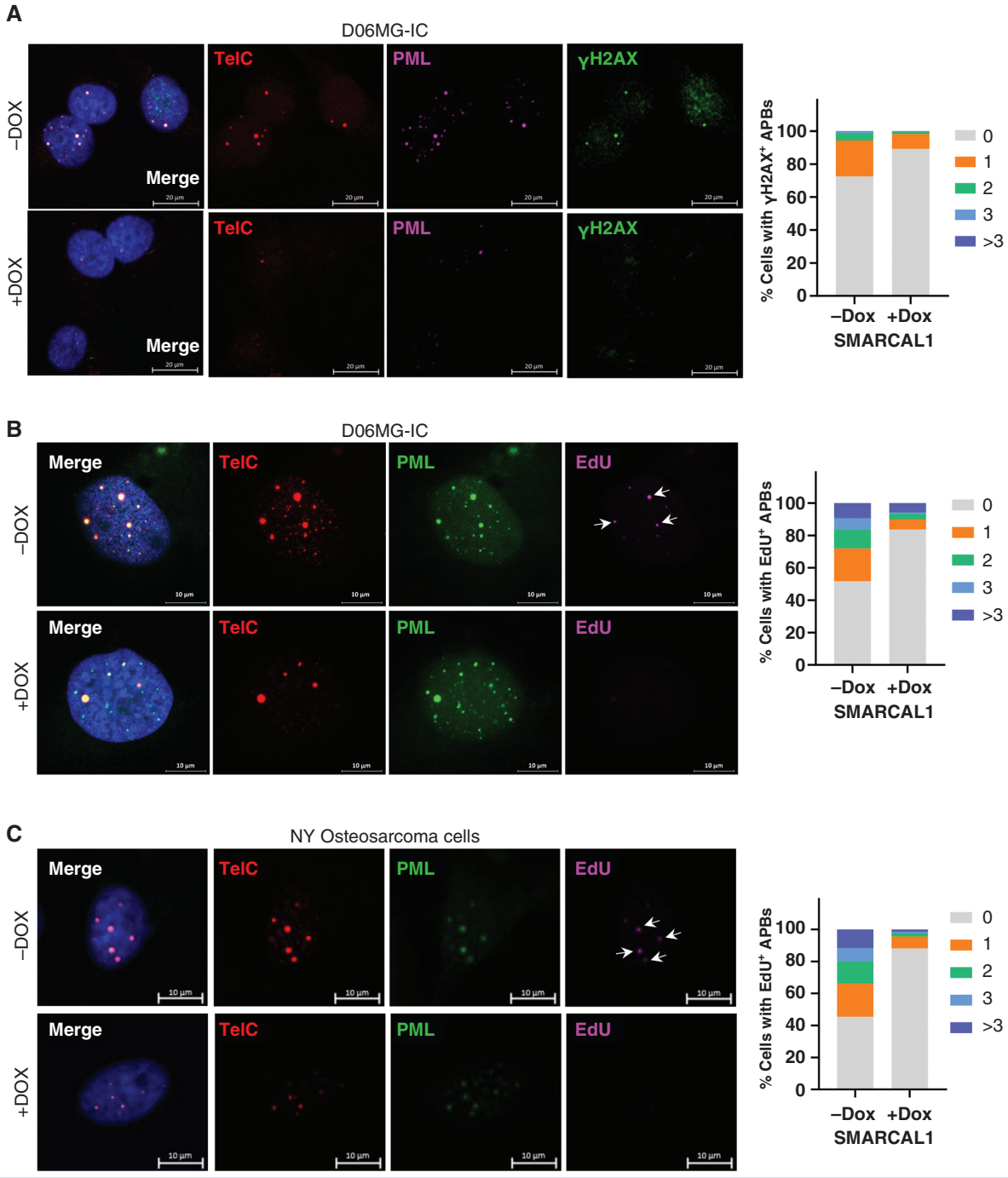

Figure 5. SMARCAL1 activity suppresses telomeric DNA double-strand breaks and de novo telomere synthesis in D06MG cells. (**A**) D06MG-IC cells without or with doxycycline-inducible SMARCAL1 rescue were analyzed for associated PML bodies (APBs) and γH2AX abundance. Representative images are shown. Cells were cultured in a chamber slide and SMARCAL1 expression was induced with doxycycline (1 ug/ml for 5 days). Cells were fixed and processed for IF-FISH with a TelC probe, anti-γH2AX antibody, and anti-PML antibody. Bar graph depicts the proportion of nuclei that exhibit APBs with co-staining of γH2AX. (**B**) D06MG-IC cells without or with doxycycline-induced SMARCAL1 expression were pulse-labeled with EdU (2 hours) before processing for IF-FISH detection of APBs and EdU foci. EdU staining at APBs was used to detect nascent telomeric DNA synthesis. (**C**) Experiment performed as in (B) with NY osteosarcoma cells.

induction caused by perturbations in histone deposition. However, based on published studies and our results, we speculate that the common feature of proteins whose loss-of-function leads to ALT is an ability to promote replication fork stability within difficult-to-replicate DNA sequences (ie, telomeres), thereby preventing stalled replication forks from deteriorating into DNA DSBs.[19,34,44,45] We propose that in the absence of SMARCAL1 activity, there is an increased

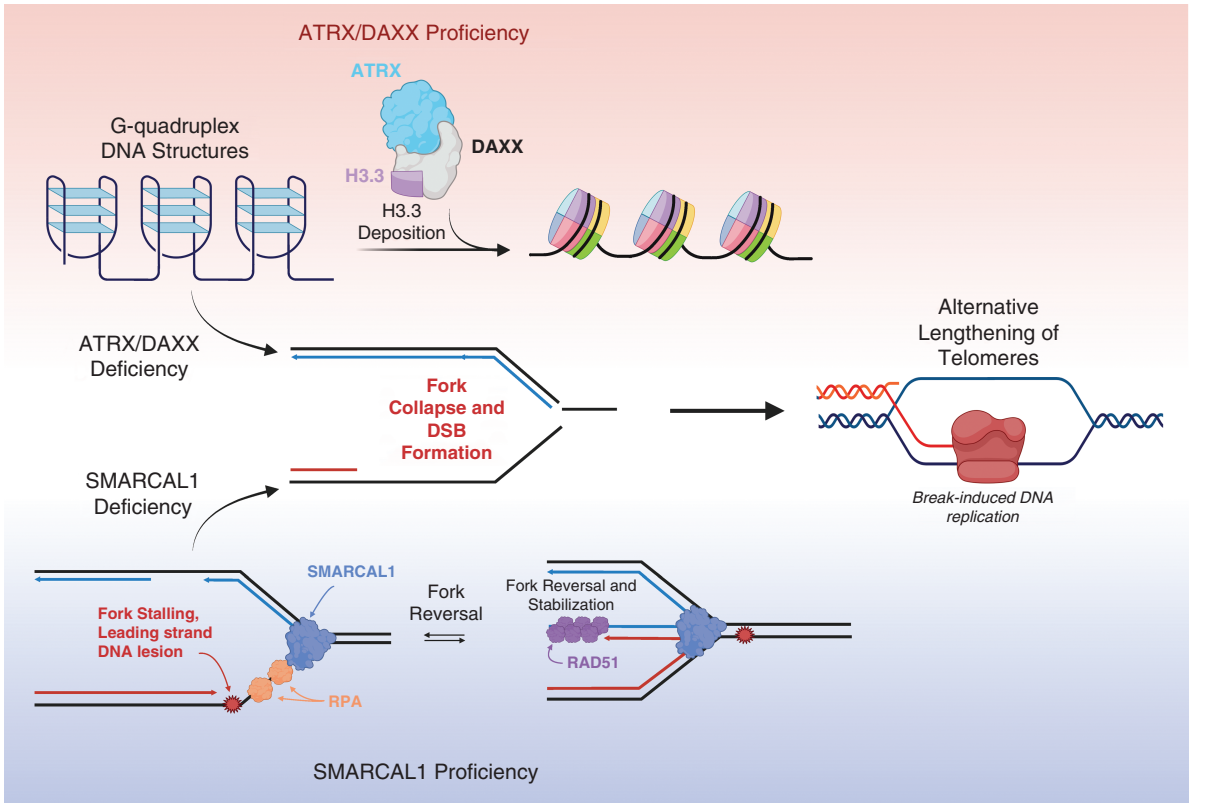

Figure 6. Alternative pathways of alternative lengthening of telomeres (ALT) induction in human cancers. Cancer-associated loss-of-function genetic alterations occurring in ATRX/DAXX (top) or SMARCAL1 (bottom) can independently lead to ALT induction in cancer cells. ATRX/DAXX deficiency compromises the canonical H3.3 chaperone function of these proteins, leading to increased G-quadruplex formation and replication stress at telomeres. SMARCAL1 deficiency leads to a loss of replication fork reversal and stabilization, thus leading to degeneration into double-strand breaks, which in turn facilitate break-induced replication of telomeres. Illustration was created with Biorender.com.

frequency of stalled replication forks within telomeric DNA that collapse into single and double-stranded DNA breaks and that this increase in telomeric DSBs functions as a nexus for break-induced replication of telomeres (Figure 6).[8,18,44,46–48]

Although we have shown that SMARCAL1 deficiency contributes to ALT induction in a subset of *ATRX* wild-type GBMs, SMARCAL1 activity has also been shown to play a role in resolving DNA replication stress and promoting ALT activity in the ATRX-deficient setting. Cox et al. have shown that SMARCAL1 localizes to APBs in ATRX-deficient ALT-positive sarcoma cells.[39] In that study, the investigators showed that SMARCAL1 activity prevents excessive replication fork stalling at ALT telomeres, thereby inhibiting DSB formation and preventing chromosomal fusions.[39] SMARCAL1 may therefore exhibit a dual function in telomere maintenance in the context of ALT. In the ATRX-deficient context (ATRX-deficient ALT), SMARCAL1 activity appears to be critical for maintaining relative genome stability and promoting telomere maintenance.[39] On the other hand, *SMARCAL1* loss-of-function genetic alterations contribute to ALT-mediated telomere maintenance (SMARCAL1-deficient ALT) in tumors and cell lines that express wild-type ATRX.[2,25] Importantly, the molecular mechanisms of ATRX-deficient ALT and SMARCAL1-deficient ALT must be at least partially distinct, as SMARCAL1 activity plays a critical role in resolving replication stress in the ATRX-deficient setting that, by definition, SMARCAL1 cannot perform in the SMARCAL1-deficient ALT context. The extent to which SMARCAL1-deficient ALT and ATRX-deficient ALT exhibit common and unique mechanisms of telomere synthesis and resolution of replication stress will be investigated in future studies.

The availability of patient-derived ATRX-deficient ALT cell lines and xenografts has been historically limited for a number of reasons. First, the majority of ALT-positive adult glioma cases occur in *IDH*-mutant astrocytomas (grades 2–4), which have been challenging to establish as cultured cell lines.[49] Those lines that have been established are almost invariably derived from recurrent cases that have progressed to high-grade tumors and are often pretreated with TMZ and/or radiotherapy.[28,49] Moreover, because *ATRX* encodes a large protein, it is difficult to develop experimental models with rescued ATRX expression to dynamically regulate the ALT phenotype. Our D06MG models are therefore unique in that they are ALT-positive GBM cells that are derived from an untreated primary tumor.[2] Further, because SMARCAL1 is a relatively small protein compared to ATRX, inducible rescue of SMARCAL1 expression is

feasible in these cells, allowing the dynamic modulation of the ALT phenotype in vitro and in vivo (Figures 4 and 5). We propose that modulating ALT in this isogenic context may be valuable for future studies aimed at further understanding the molecular mechanisms of ALT and for identifying novel anticancer therapeutics that target the ALT phenotype.

In summary, our results demonstrate that SMARCAL1-deficiency promotes ALT-mediated telomere maintenance in a manner that supports tumorigenesis in a patient-derived xenograft model. Although the majority of ALT-positive tumors and cell lines are ATRX-deficient, the underlying genetics and mutational status of *SMARCAL1* and *ATRX* should be considered in future preclinical and clinical studies that focus on ALT mechanisms and associated drug sensitivities. Finally, SMARCAL1-deficient ALT-positive models may be useful tools for transiently suppressing the ALT phenotype or phenotype-switching (ALT to telomerase) to create isogenic model systems comparing therapeutic vulnerabilities according to telomere maintenance mechanisms.[9]

Supplementary material

Supplementary material is available online at *Neuro-Oncology* (http://neuro-oncology.oxfordjournals.org/).

Keywords

Adult gliomas | alternative lengthening of telomeres | ATRX | gliomagenesis | SMARCAL1 | telomere maintenance

Funding

This work was supported by The Preston Robert Tisch Brain Tumor Center and NIH grant 1K22CA258965-01A1 awarded to M.S.W.

Acknowledgments

We thank Drs. Lisa Cameron and Yasheng Gao of the Duke Light Microscopy Core Facility for imaging support and expertise, Drs. So Young Kim, Sufeng Li, and Vidya Seshadri of the Duke Functional genomics Core for their help with generating constructs used in the study, Dr. Wenxia Jiang of the Herbert Irving Comprehensive Cancer Center (HICCC) Cytogenetics Core, Columbia University, for cytogenetic analysis, and Dr. Hai Yan for his guidance and resources during the early stages of this work. We thank the staff of the Cancer Center Isolation Facility (CCIF), Duke Cancer Institute, for assistance with the in vivo experiments. This work was supported by The Preston Robert Tisch Brain Tumor Center and NIH grant 1K22CA258965-01A1 awarded to M.S.W.

Conflict of interest statement

None to disclose.

Author Contributions

Conceptualization: Heng Liu, Bill Diplas, Matthew Waitkus. Data curation: Heng Liu, Yiping He, Stephen Keir, Matthew Waitkus. Funding acquisition: David Ashley, Matthew Waitkus. Investigation: Heng Liu, Cheng Xu, Alexandrea Brown, Laura Strickland, Haipei Yao, Jinjie Ling, Stephen Keir, Matthew Waitkus. Methodology: Heng Liu, Cheng Xu, Bill Diplas, Stephen Keir, David Ashley, Matthew Waitkus. Resources: Stephen Keir, Roger McLendon, David Ashley, Matthew Waitkus. Supervision: Yiping He, Matthew Waitkus. Writing – original draft: Heng Liu, Yiping He, Matthew Waitkus. Writing – review & editing: Heng Liu, Cheng Xu, Bill Diplas, Alexandrea Brown, Laura Strickland, Jinjie Ling, Roger McLendon, Stephen Keir, David Ashley, Yiping He, Matthew Waitkus.

Affiliations

The Preston Robert Tisch Brain Tumor Center, Duke University Medical Center, Durham, North Carolina, USA (H.L., C.X., B.H.D., A.B., L.M.S., H.Y., J.L., R.E.M., S.T.K., D.M.A., Y.H., M.S.W.); Department of Pathology, Duke University Medical Center, Durham, North Carolina, USA (H.L., C.X., B.H.D., H.Y., J.L., R.E.M., Y.H.); Department of Neurosurgery, Duke University Medical Center, Durham, North Carolina, USA (A.B., L.M.S., S.T.K., D.M.A., M.S.W.)

References

1. Killela PJ, Reitman ZJ, Jiao Y, et al. TERT promoter mutations occur frequently in gliomas and a subset of tumors derived from cells with low rates of self-renewal. *Proc Natl Acad Sci U S A.* 2013;110(15):6021–6026.
2. Diplas BH, He X, Brosnan-Cashman JA, et al. The genomic landscape of TERT promoter wildtype-IDH wildtype glioblastoma. *Nat Commun.* 2018;9(1):2087.
3. Walsh KM, Wiencke JK, Lachance DH, et al. Telomere maintenance and the etiology of adult glioma. *Neuro Oncol.* 2015;17(11):1445–1452.
4. Dunham MA, Neumann AA, Fasching CL, Reddel RR. Telomere maintenance by recombination in human cells. *Nat Genet.* 2000;26(4):447–450.
5. Cesare AJ, Kaul Z, Cohen SB, et al. Spontaneous occurrence of telomeric DNA damage response in the absence of chromosome fusions. *Nat Struct Mol Biol.* 2009;16(12):1244–1251.
6. Heaphy CM, de Wilde RF, Jiao Y, et al. Altered telomeres in tumors with ATRX and DAXX mutations. *Science.* 2011;333(6041):425425.–4254425.
7. Pickett HA, Reddel RR. Molecular mechanisms of activity and derepression of alternative lengthening of telomeres. *Nat Struct Mol Biol.* 2015;22(11):875–880.

8. Lu R, Pickett HA. Telomeric replication stress: the beginning and the end for alternative lengthening of telomeres cancers. *Open Biol.* 2022;12(3).
9. Gao J, Pickett HA. Targeting telomeres: advances in telomere maintenance mechanism-specific cancer therapies. *Nat Rev Cancer.* 2022;22(9):515–532.
10. Mangerel J, Price A, Castelo-Branco P, et al. Alternative lengthening of telomeres is enriched in, and impacts survival of TP53 mutant pediatric malignant brain tumors. *Acta Neuropathol.* 2014;128(6):853–862.
11. Heaphy CM, Subhawong AP, Hong SM, et al. Prevalence of the alternative lengthening of telomeres telomere maintenance mechanism in human cancer subtypes. *Am J Pathol.* 2011;179(4):1608–1615.
12. Jiao Y, Killela PJ, Reitman ZJ, et al. Frequent ATRX, CIC, FUBP1, and IDH1 mutations refine the classification of malignant gliomas. *Oncotarget.* 2012;3(7):709–722.
13. Brat DJ, Verhaak RGW, Aldape KD, et al; Cancer Genome Atlas Research NetworkCancer Genome Atlas Research Network. Comprehensive, integrative genomic analysis of diffuse lower-grade gliomas. *N Engl J Med.* 2015;372(26):2481–2498.
14. Reinhardt A, Stichel D, Schrimpf D, et al. Anaplastic astrocytoma with piloid features, a novel molecular class of IDH wildtype glioma with recurrent MAPK pathway, CDKN2A/B and ATRX alterations. *Acta Neuropathol.* 2018;136(2):273–291.
15. Rodriguez FJ, Brosnan-Cashman JA, Allen SJ, et al. Alternative lengthening of telomeres, ATRX loss and H3-K27M mutations in histologically defined pilocytic astrocytoma with anaplasia. *Brain Pathol.* 2019;29(1):126–140.
16. Khuong-Quang DA, Buczkowicz P, Rakopoulos P, et al. K27M mutation in histone H3.3 defines clinically and biologically distinct subgroups of pediatric diffuse intrinsic pontine gliomas. *Acta Neuropathol.* 2012;124(3):439–447.
17. Dorris K, Sobo M, Onar-Thomas A, et al. Prognostic significance of telomere maintenance mechanisms in pediatric high-grade gliomas. *J Neurooncol.* 2014;117(1):67–76.
18. Dilley RL, Verma P, Cho NW, et al. Break-induced telomere synthesis underlies alternative telomere maintenance. *Nature.* 2016;539(7627):54–58.
19. Zhang JM, Zou L. Alternative lengthening of telomeres: from molecular mechanisms to therapeutic outlooks. *Cell Biosci.* 2020;10(1):1–9.
20. Dyer MA, Qadeer ZA, Valle-Garcia D, Bernstein E. ATRX and DAXX: mechanisms and mutations. *Cold Spring Harb Perspect Med.* 2017;7(3):a026567.
21. Bansbach CE, Bétous R, Lovejoy CA, Glick GG, Cortez D. The annealing helicase SMARCAL1 maintains genome integrity at stalled replication forks. *Genes Dev.* 2009;23(20):2405–2414.
22. Bétous R, Mason AC, Rambo RP, et al. SMARCAL1 catalyzes fork regression and holliday junction migration to maintain genome stability during DNA replication. *Genes Dev.* 2012;26(2):151–162.
23. Berti M, Cortez D, Lopes M. The plasticity of DNA replication forks in response to clinically relevant genotoxic stress. *Nat Rev Mol Cell Biol.* 2020;21(10):633–651.
24. Brosnan-Cashman JA, Davis CM, Diplas BH, et al. SMARCAL1 loss and alternative lengthening of telomeres (ALT) are enriched in giant cell glioblastoma. *Mod Pathol.* 2021;34(10):1810–1819.
25. Mason-Osann E, Dai A, Floro J, et al. Identification of a novel gene fusion in ALT positive osteosarcoma. *Oncotarget.* 2018;9(67):32868–32880.
26. de Nonneville A, Salas S, Bertucci F, et al. TOP3A amplification and ATRX inactivation are mutually exclusive events in pediatric osteosarcomas using ALT. *EMBO Mol Med.* 2022;14(10):e15859.
27. Akhavanfard S, Padmanabhan R, Yehia L, Cheng F, Eng C. Comprehensive germline genomic profiles of children, adolescents and young adults with solid tumors. *Nat Commun.* 2020;11(1):2206.
28. Waitkus MS, Pirozzi CJ, Moure CJ, et al. Adaptive evolution of the GDH2 allosteric domain promotes gliomagenesis by resolving IDH1R132H-induced metabolic liabilities. *Cancer Res.* 2018;78(1):36canres.1352.2017–36canres.1352.2050.
29. Ritchie ME, Phipson B, Wu D, et al. limma powers differential expression analyses for RNA-sequencing and microarray studies. *Nucleic Acids Res.* 2015;43(7):e47.
30. Love MI, Huber W, Anders S. Moderated estimation of fold change and dispersion for RNA-seq data with DESeq2. *Genome Biol.* 2014;15(12):550.
31. Liao Y, Smyth GK, Shi W. an efficient general purpose program for assigning sequence reads to genomic features. *Bioinformatics.* 2014;30(7):923–930.
32. Alhamdoosh M, Ng M, Wilson NJ, et al. Combining multiple tools outperforms individual methods in gene set enrichment analyses. *Bioinformatics.* 2017;33(3):414–424.
33. Oeck S, Malewicz NM, Hurst S, et al. The focinator v2-0 - graphical interface, four channels, colocalization analysis and cell phase identification. *Radiat Res.* 2017;188(1):114–120.
34. Zhang J, Yadav T, Ouyang J, Lan L, Zou L. Alternative lengthening of telomeres through two distinct break-induced replication pathways. *Cell Rep.* 2019;26(4):955–968.e3.
35. Liberzon A, Birger C, Thorvaldsdóttir H, et al. The molecular signatures database hallmark gene set collection. *Cell Syst.* 2015;1(6):417–425.
36. Gao XD, Tu LC, Mir A, et al. C-BERST: defining subnuclear proteomic landscapes at genomic elements with dCas9-APEX2. *Nat Methods.* 2018;15(6):433–436.
37. Lu R, O'Rourke JJ, Sobinoff AP, et al. The FANCM-BLM-TOP3A-RMI complex suppresses alternative lengthening of telomeres (ALT). *Nat Commun.* 2019;10(1).
38. Couch FB, Bansbach CE, Driscoll R, et al. ATR phosphorylates SMARCAL1 to prevent replication fork collapse. *Genes Dev.* 2013;27(14):1610–1623.
39. Cox KE, Maréchal A, Flynn RL. SMARCAL1 resolves replication stress at ALT telomeres. *Cell Rep.* 2016;14(5):1032–1040.
40. O'Sullivan RJ, Arnoult N, Lackner DH, et al. Rapid induction of alternative lengthening of telomeres by depletion of the histone chaperone ASF1. *Nat Struct Mol Biol.* 2014;21(2):167–174.
41. Yusufzai T, Xiangduo K, Kyoko Y, Kadonaga JT. The annealing helicase HARP is recruited to DNA repair sites via an interaction with RPA. *Genes Dev.* 2009;23(20):2400–2404.
42. Ciccia A, Bredemeyer AL, Sowa ME, et al. The SIOD disorder protein SMARCAL1 is an RPA-interacting protein involved in replication fork restart. *Genes Dev.* 2009;23(20):2415–2425.
43. Panier S, Maric M, Hewitt G, et al. SLX4IP antagonizes promiscuous BLM activity during ALT maintenance. *Mol Cell.* 2019;76(1):27–43.e11.
44. Zhao Y, Zhang Z, Shengzhao G, et al. Strand break-induced replication fork collapse leads to C-circles, C-overhangs and telomeric recombination. *PLoS Genet.* 2019;15(2):e1007925.
45. Episkopou H, Draskovic I, Van Beneden A, et al. Alternative lengthening of telomeres is characterized by reduced compaction of telomeric chromatin. *Nucleic Acids Res.* 2014;42(7):4391–4405.
46. Sobinoff AP, Pickett HA. Alternative lengthening of telomeres: DNA repair pathways converge. *Trends Genet.* 2017;33(12):921–932.
47. Roumelioti F, Sotiriou SK, Katsini V, et al. Alternative lengthening of human telomeres is a conservative DNA replication process with features of break- induced replication. *EMBO Rep.* 2016;345(6274):e201643169.
48. Le S, Moore JK, Haber JE, Greider CW. RAD50 and RAD51 define two pathways that collaborate to maintain telomeres in the absence of telomerase. *Genetics.* 1999;152(1):143–152.
49. Wakimoto H, Tanaka S, Curry WT, et al. Targetable signaling pathway mutations are associated with malignant phenotype in IDH-mutant gliomas. *Clin Cancer Res.* 2014;20(11):2898–2909.